EFFECT OF DILUTE SOLID PHASE ON THE MAGNITUDE OF ACCELERATION TERM OF TOTAL PRESSURE DROP IN HORIZONTAL GAS PIPES

VICTOR JOSEPH AIMIKHE [*1], TIYA KRISTIANA WEST [1]

[1]Department of Petroleum and Gas Engineering, University of Port Harcourt, Choba, Rivers, Nigeria

Abstract: In this study, the effect of dilute solid phase on the magnitude of acceleration term of total pressure drop in horizontal gas pipes is investigated. The percentage contribution of pressure drop due to acceleration to the total pressure drop was studied at different pipe diameters, pipe lengths, solid concentrations, and solid-gas density ratios, respectively. The results showed that the contribution of pressure drop due to acceleration to the total pressure drop for gas-solid systems could generally be considered insignificant (less than 1%).

Keywords: gas-solid flow, horizontal pipe, pressure drop, acceleration term

1. INTRODUCTION

The flow of gases and solid particles in pipes is an everyday occurrence in our daily life. Two-phase flow has attracted significant interest in many industries, including food production and processing, petroleum, power generation, and chemical plants [1]. When reservoir fluids are transported for processing through pipelines, sand, and most times, fines and the fluid settles in the lower part of the pipes to form beds along the bottom of the line if the velocity is less than the minimum solids transport velocity required [2]. Likewise, the presence of crystals of hydrates, paraffin, asphaltenes, and other debris like black powder can constitute solid loading phase in the gas stream during transportation. In other applications, pneumatic conveying of particles or other tiny solids in channel or pipe flows is of great technical importance. It is characterized by particle-phase segregations primarily due to gravity and particle inertia. In such applications, gas can be used to transport sand or even fines through pipelines.

Consequently, numerous researchers have been curious about gas-solid flow because it is thought to provide a convenient way to transport solids [3]. Due to solid loading, pipeline problems affect the total pressure drop in pipes and may become severe in gas transportation. Sand accumulation in the pipeline may lead to partial or complete blockage of the pipe. It is one of the major problems in the petroleum industry. It results in a rapid increase in the cost of pump maintenance, well-cleaning, disposal of dirty sands, and workover operations. Sand transportation, either during injection or production, also results in excessive drops in pressure, equipment failure, corrosion of pipe, production decrease, and unexpected downtime [4]. Removing these solid quantities is often problematic and challenging, and often time-consuming.

Hence the need for pre-filtering equipment in many industries, including food, cement, oil and gas refining, ventilating, and air conditioning [5]. These problems can be minimized or controlled by understanding the mechanism of particle transportation in different flow regimes and considering the various parameters like pipe diameter and flow rate when observing the minimum critical velocity at which the particles start flowing [6]. Small particles can become stationary if gas velocity or pressure (gas density) is small enough [7]. One arduous task is

[*] Corresponding author, email: victor.aimikhe@uniport.edu.ng https://doi.org/10.29081/jesr.v29i3.001

continuously transporting the multiphase fluids without particles depositing on the pipe surface. Doing this requires a clear understanding of multiphase flow- regimes and the effects of particle transport. One way to investigate the flow of gases in pipes is by measuring pressure losses.

In horizontal pipe calculations, friction and acceleration are essential in determining a pipe's pressure losses. However, many existing pressure drop studies on solid-gas flow focused on analyzing the frictional component of total pressure drop, neglecting the acceleration component [8–10]. Scant attention has been given to the acceleration component in horizontal gas pipelines. Where such studies exist, the emphasis has been mainly on single-phase gas flow. Published results have shown that neglecting the acceleration component while estimating total pressure losses for gas flow can be misleading [11-14]. Furthermore, the scarce studies on gas-solid diphasic flow did not investigate solid particles' influence on the acceleration term's magnitude. That is, they did not consider the influence of the solids on the magnitude of the acceleration term component of the pressure drop. This study becomes imperative for comprehensively understanding gas-solid horizontal flow and accurately estimating its total pressure drop.

2. DESCRIPTION OF MATHEMATICAL MODEL

2.1. Gas-solid flow rate model development

Using the general energy equation, the Energy balance on the whole system between points 1 and 2 in Figure 1 below may be written as:

$$u_2 + p_2 v_2 + \frac{mu_2^2}{2g_c} + \frac{mgz_2}{g_c} = u_1 + p_1 v_1 + \frac{mu_1^2}{2g_c} + \frac{mgz_1}{g_c} + Q - w - lw \tag{1}$$

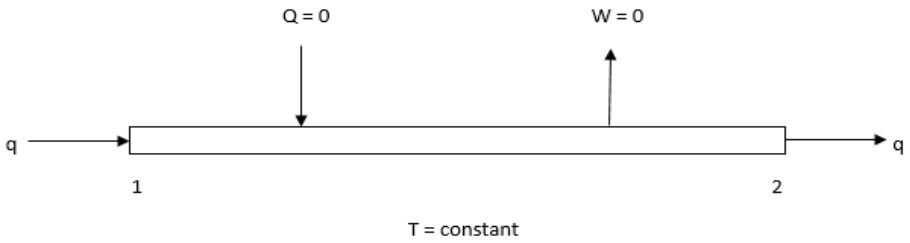

Fig. 1. A gas transmission line model [14].

where *U* are internal energy, *PV* is energy of compression or expansion, $\frac{mu^2}{2g_c}$ is potential energy, *Q is* heat energy added to the fluid, *W* is shaft work done by the surrounding on the gas.

Dividing equation (1) through by m to obtain an energy per unit mass balance and writing the resulting equation in differential form yields:

$$dU + d\left(\frac{p}{\rho}\right) + u\left(\frac{du}{g_c}\right) + g\frac{dz}{g_c} + dQ - dw = 0 \tag{2}$$

Assuming the following:

(a) The flow is steady state and steady flow;
(b) The flow is isothermal in the pipeline;
(c) The flow is horizontal;
(d) There is no work done by or on the gas during flow across the system.

But,

$$dh = Tds + \frac{dP}{\rho}$$

and

$$dU = dh - d\left(\frac{P}{\rho}\right)$$

$$= Tds + \frac{dP}{\rho} - d\left(\frac{P}{\rho}\right) \quad (3)$$

where h are enthalpy, s is entropy, T is temperature, ρ is density, P is gas pressure, U is internal energy.

Inserting equation (3) into (2):

$$Tds + \frac{dP}{\rho} + u\frac{du}{g_c} + g\frac{dz}{g_c} + dQ - dw = 0 \quad (4)$$

Clausis inequality for an irreversible process states that:

$$ds \geq \frac{-dQ}{T}$$

$$Tds = -dQ + d(lw) \quad (5)$$

where lw are lost work due to irreversibilities.

Substituting equation (5) into (4):

$$\frac{dP}{\rho} + u\frac{du}{g_c} + g\frac{dz}{g_c} + d(lw) - dw = 0 \quad (6)$$

If no work is done by or on the fluid, $dw = 0$

Then,

$$\frac{dP}{\rho} + u\frac{du}{g_c} + g\frac{dz}{g_c} + d(lw) = 0 \quad (7)$$

Considering a more general case of an inclined pipe we have:

$$\frac{dP}{\rho} + u\frac{du}{g_c} + g\frac{dL\sin\theta}{g_c} + d(lw) = 0 \quad (8)$$

Multiplying through by $\frac{\rho}{dL}$:

$$\frac{dP}{dL} + \rho u\frac{du}{g_c dL} + g\frac{\rho\sin\theta}{g_c} + \rho\frac{d(lw)}{dL} = 0 \quad (9)$$

where $\frac{d(lw)}{dL} = \frac{fu^2}{2g_c D}$.

Considering pressure drop in the positive direction and substituting:

$$\frac{dP}{dL} = \rho u\frac{du}{g_c dL} + g\frac{\rho\sin\theta}{g_c} + \rho\frac{fu^2}{2g_c D} \quad (10)$$

Considering a horizontal pipe:

$$\frac{dP}{dL} = \rho u\frac{du}{g_c dL} + \rho\frac{fu^2}{2g_c D} \quad (11)$$

Recall:

$$u = \left(\frac{q}{86400}\right)\left(\frac{T}{T_b}\right)\left(\frac{p_b}{p}\right)\left(\frac{z}{1.00}\right)\left(\frac{4}{\pi D^2}\right) \quad (12)$$

where q are volumetric flow rate, scfd measured at standard conditions, T_b (°R) and P_b (psia).

But, the total surface area of a cylinder = Area of the two circular ends + Area of the curved surface.

$$A_t = 2\pi r^2 + 2\pi rL$$

where L are length of pipe.

But for an open-ended flowing pipe:

$$A = 2\pi rL$$

So that:

$$r = \frac{A}{2\pi L}$$

Hence:

$$\pi\left(\frac{D}{2}\right)^2 = \pi\left(\frac{A}{2\pi L}\right)^2 = \frac{A^2}{4\pi L^2} \tag{13}$$

Substituting equation (13) into equation (12):

$$u = \left(\frac{q}{86400}\right)\left(\frac{T}{T_b}\right)\left(\frac{p_b}{p_{ave}}\right)\left(\frac{z}{1.00}\right)\left(\frac{4\pi L^2}{A^2}\right) \tag{14}$$

But:

$$\frac{\partial u}{\partial L} = \left(\frac{q}{86400}\right)\left(\frac{T}{T_b}\right)\left(\frac{p_b}{p_{ave}}\right)\left(\frac{z}{1.00}\right)\left(\frac{8\pi L}{A^2}\right)$$

Then, let:

$$\frac{\partial u}{\partial L} \approx \frac{du}{dL}$$

So that:

$$\frac{\partial u}{\partial L} = \left(\frac{q}{10800}\right)\left(\frac{T}{T_b}\right)\left(\frac{p_b}{p_{ave}}\right)\left(\frac{z}{1.00}\right)\left(\frac{\pi L}{A^2}\right) = \frac{2u}{L} \tag{15}$$

Substituting equation (15) into equation (11):

$$\frac{dP}{dL} = 2\rho\frac{u^2}{g_c L} + \rho\frac{fu^2}{2g_c D} \tag{16}$$

Meanwhile, acceleration causes a pressure drop in the direction of velocity increase for a compressible fluid, bringing about kinetic change or acceleration effects. The pressure of particles will cause a difference in velocity (slip) in the two-phase fluid- flow, contributing to a pressure drop. Pressure at the start and end of the pipe is required for the flow rate calculations. Other parameters are pipe diameter, pipe length, fluid density, viscosity, and particle concentrations. The pressure difference in the pipe due to the change in height is assumed negligible. An application of mixture theory combining gas and solids is considered. Since solid particles are small, and gas is the continuous phase, gas velocity will adequately overcome the terminal settling velocity of the solids. Hence, $\mathbf{V}_g = \mathbf{V}_t$. The theoretical analysis and mathematical model for the combined gas-solid flow system (Figure 2) were developed under the flowing assumptions:

1. The flow is steady-state and steady-flow;
2. The flow is isothermal in the pipeline;
3. The flow is horizontal;
4. There is no work done by or on gas during flow-across system.

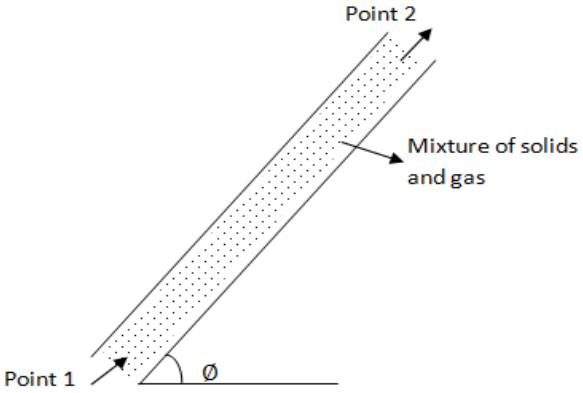

Fig. 2. Flow of a mixture of gas and solid in an inclined pipe [15].

According to mixture theory [15], the combined flow of gas-solids experiences a total pressure drop given by:

$$\left(\frac{dp}{dl}\right)_{mixture}^{total} = (1-\beta)\left(\frac{dp}{dl}\right)_{gas}^{total} + \beta\left(\frac{dp}{dl}\right)_{solid}^{total} \tag{17}$$

The total pressure drop in a gas pipeline is given as [16]:

$$\left(\frac{dp}{dl}\right)_{gas}^{total} = \left(\frac{dp}{dl}\right)_{friction} + \left(\frac{dp}{dl}\right)_{elevation} + \left(\frac{dp}{dl}\right)_{acceleration} \tag{18}$$

The above equation is fully expressed as:

$$\left(\frac{dp}{dl}\right)_{gas}^{total} = \frac{\rho u du}{g_c dL} + g\frac{\rho_s \sin\theta}{g_c} + \frac{\rho f u^2}{2g_c D} \tag{19}$$

From equation (16), equation (18) can be expressed as follows for inclined pipes

$$\left(\frac{dp}{dl}\right)_{gas}^{total} = 2\rho_g \frac{u^2}{g_c L} + \frac{g\rho_g \sin\theta}{g_c} + \frac{\rho f_g u^2}{2g_c D} \tag{20}$$

or

$$\left(\frac{dp}{dl}\right)_{gas}^{total} = \frac{\rho u^2}{g_c}\left(\frac{2}{L} + \frac{f}{2D}\right) + \frac{g\rho_g \sin\theta}{g_c} \tag{21}$$

Similarly, according to Ortega-rivas [17], the total pressure drop for particulate solids transported pneumatically in inclined pipes is also given by:

$$\left(\frac{dp}{dl}\right)_{solid}^{total} = \left(\frac{dp}{dl}\right)_{friction} + \left(\frac{dp}{dl}\right)_{elevation} + \left(\frac{dp}{dl}\right)_{acceleration} \tag{22}$$

Which is fully expressed as:

$$\left(\frac{dp}{dl}\right)_{solids}^{total} = \frac{\rho_s {u_p}^2}{g_c} + \frac{\rho_s g \sin\theta}{g_c} + \frac{\pi}{8}\left(\frac{f_s}{f_g}\right)\left(\frac{\rho_s}{\rho_g}\right)^{1/2}\left(\frac{G_s}{G}\right)E_g \tag{23}$$

where:

$$E_g = \frac{\rho_g f_g u^2}{2 g_c D}$$

Considering a pipe section in Figure 3 with solid (particle) and gas concentration and combining equations (20) and (23).

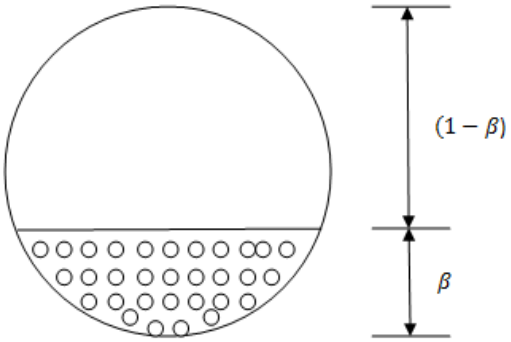

Fig. 3. Cross-section of pipe showing the solid volumetric concentration β.

$$\left(\frac{dp}{dl}\right)_{mixture}^{total} = (1-\beta)\left\{2\rho_g \frac{u^2}{g_c L} + \rho \frac{f_g u^2}{2 g_c D} + \frac{g \rho_g \sin\theta}{g_c}\right\} + \beta\left\{\frac{\rho_s u_p^2}{g_c} + \frac{\rho_s g \sin\theta}{g_c} + \frac{\pi}{8}\left(\frac{f_s}{f_g}\right)\left(\frac{\rho_s}{\rho_g}\right)^{1/2} \frac{G_s}{G} \frac{\rho_g f_g u^2}{2 g_c D}\right\} \quad (24)$$

where β are solid-volumetric-concentration (-), U_p *is* particle-velocity relative to gas-velocity(ft/s), $u_p = u - u_t$, with u is gas-velocity (ft/s), u_t is terminal setting velocity(ft/s) of a particle given by:

$$u_t = \frac{x_p^2(\rho_s - \rho_g)g}{18 \mu_g g_c} \quad (25)$$

where f_s= particle-friction-factor (-), $f_g$is moody friction-factor (-), G_s is flux of solid particles (lbm/ft^{2}s), G_s is $p_s u_p$, G is flux of gas, G = $\rho_g u$, D is pipe-diameter(in), L is pipe-length (ft), A_t= total-surface area of pipe = $\pi D(r + l)$, g_c= conversion-factor = 32.17 lbm-ft/ bf-S^2, π= 3.1428571429, ρ_g is gas density (lbm/ft^3), ρ_s is particle density (lbm/ft^3), x_p is particle diameter (ft), u_g *is* gas viscosity (cp).

Assuming gas velocity just equals the particle's terminal settling velocity in horizontal gas pipes, equation (24) reduces to:

$$\left(\frac{dp}{dl}\right)_{mixture}^{total} = (1-\beta)\left\{2\rho_g \frac{u^2}{g_c L} + \rho \frac{f_g u^2}{2 g_c D}\right\} + \beta\left\{\frac{\pi}{8}\left(\frac{f_s}{f_g}\right)\left(\frac{\rho_s}{\rho_g}\right)^{1/2} \frac{G_s}{G} \frac{\rho_g f_g u^2}{2 g_c D}\right\} \quad (26)$$

On further simplification,

$$\left(\frac{dp}{dl}\right)_{mixture}^{total} = (1-\beta)2\rho_g \frac{u^2}{g_c L} + (1-\beta)\frac{\rho_g u^2 f_g}{2 g_c D} + \frac{\beta\pi}{8}\left(\frac{f_s}{f_g}\right)\left(\frac{\rho_s}{\rho_g}\right)^{1/2}\left(\frac{G_s}{G}\right)\frac{\rho_g f_g u^2}{2 g_c D} \quad (27)$$

Recall that,

$$G = \rho u \quad (28)$$

so that,

$$\frac{G_s}{G} = \frac{\rho_s u_p}{\rho_g u} \quad (29)$$

But for steady-state flow $u_p = u$ so that,

$$\frac{G_S}{G} = \frac{\rho_S}{\rho_g} \tag{30}$$

Substituting equation (30) into (27) and changing, $\frac{dp}{dl} to \frac{\Delta p}{L}$ we have:

$$\frac{\Delta p}{L} = (1-\beta)2\rho_g \frac{u^2}{g_c L} + (1-\beta)\frac{\rho_g u^2 f_g}{2g_c D} + \frac{\beta\pi}{8}\left(\frac{f_s}{f_g}\right)\left(\frac{\rho_s}{\rho_g}\right)^{3/2}\frac{\rho_g f_g u^2}{2g_c D} \tag{31}$$

2.2. Ratio of pressure drop due to acceleration to total pressure drop

The ratio of pressure drop due to acceleration to total pressure drop can be defined as

$$\varpi = \frac{\text{Pressure drop due to acceleration}}{\text{Total pressure drop}} \tag{32}$$

From equation (31), the total pressure drop given for horizontal pipes is:

$$\left(\frac{dp}{dl}\right)_{mixture}^{total} = (1-\beta)2\rho_g \frac{u^2}{g_c L} + (1-\beta)\frac{\rho_g u^2 f_g}{2g_c D} + \frac{\beta\pi}{8}\left(\frac{f_s}{f_g}\right)\left(\frac{\rho_s}{\rho_g}\right)^{3/2}\frac{\rho_g f_g u^2}{2g_c D} \tag{33}$$

The pressure drop due to acceleration is given by:

$$\left(\frac{dp}{dl}\right)_{mixture}^{acceleration} = (1-\beta)2\rho_g \frac{u^2}{g_c L} \tag{34}$$

Therefore from equation (32):

$$\varpi = \frac{(1-\beta)2\rho_g \frac{u^2}{g_c L}}{(1-\beta)2\rho_g \frac{u^2}{g_c L} + (1-\beta)\frac{2\rho_g u^2 f_g}{4Dg_c} + \frac{\beta\pi}{8}\left(\frac{f_s}{f_g}\right)\left(\frac{\rho_s}{\rho_g}\right)^{3/2}\frac{2\rho_g f_g u^2}{4g_c D}}$$

$$\varpi = \frac{\frac{2\rho_g u^2}{g_c}\frac{(1-\beta)}{L}}{\frac{2\rho_g u^2}{g_c}\left\{\frac{(1-\beta)}{L} + (1-\beta)\frac{f_g}{4D} + \frac{\beta\pi}{8}\left(\frac{f_s}{f_g}\right)\left(\frac{\rho_s}{\rho_g}\right)^{3/2}\frac{f_g}{4D}\right\}}$$

$$\varpi = \frac{(1-\beta)}{L\left\{\frac{(1-\beta)}{L} + (1-\beta)\frac{f_g}{4D} + \frac{\beta\pi}{8}\left(\frac{f_s}{f_g}\right)\left(\frac{\rho_s}{\rho_g}\right)^{3/2}\frac{f_g}{4D}\right\}}$$

$$\varpi = \frac{(1-\beta)}{L\left\{\frac{(1-\beta)}{L} + (1-\beta)\frac{f_g}{4D} + \frac{\beta\pi f_s}{32D}\left(\frac{\rho_s}{\rho_g}\right)^{3/2}\right\}}$$

$$\varpi = \frac{(1-\beta)}{(1-\beta)+(1-\beta)\frac{Lf_g}{4D}+\frac{\beta\pi L f_s}{32D}\left(\frac{\rho_s}{\rho_g}\right)^{3/2}} \tag{35}$$

where ϖ are The ratio of pressure drop due to acceleration to total pressure drop in the pipe (-),L is length of pipe (ft), f_s is particle-friction-factor (-), f_g is moody friction-factor (-), D is pipe diameter (inches), β is solid-volumetric-concentration (-), ρ_g is gas density (lbm/ft^3), ρ_S is particle density (lbm/ft^3), π= 3.1428571429.

3. RESULTS AND DISCUSSION

Equations (33) and (35) and Tables 1 to 4 of the appendix were used for the result analysis of this study. From equation (33), it can be seen that the total pressure drop increases with an increase in the concentration of the solid particles. This increase in solid concentration by weight is proportional to an increase in solid density. Hence, an increase in solid density (solid loading ratio) also increases the total pressure drop. Furthermore, the model indicates that total pressure drop decreases with increasing pipe diameter. Results from the model in equation (35) are further discussed.

From the analysis of equation (35), Figure 4 shows the variation of the percentage contribution of pressure drop due to acceleration to the total pressure drop with pipe diameter at different gas friction factor values. The graph shows a generally inverse relationship between the percentage contribution of pressure drop due to acceleration and the total pressure drop and pipe diameter. It shows that the percentage contribution of pressure drop due to acceleration to the total pressure drop is less than 1%, which can be described as insignificant. The reason for this is related to the fact that since the solids entrained in the flow are fines and sands that are easily carried by a flowing gas, the buoyancy the particles experience and their dilute concentration ensures they do not significantly contribute to the overall mass of the flow. But at lower diameters, the effect of pipe diameter on the percentage contribution of pressure drop due to acceleration to the total pressure drop was significantly higher than at larger diameters. This is because reducing pipe diameter increases velocity and acceleration for a fixed flow rate, hence increasing pressure drop due to acceleration. But, for bigger diameter pipes, there is usually a larger surface area for fluid flow, and the major contributor to total pressure drop becomes pressure drop due to friction between fluid layers and friction along the pipe wall. This result is similar to the results of Okafor et al. [14], Hamad et al. [18], Saleh and Al-Byatti [19], and Santos et al. [20]. The Figure 4 also shows that the gas friction factor had no distinguishable effect on the percentage contribution of pressure drop due to acceleration to the total pressure drop.

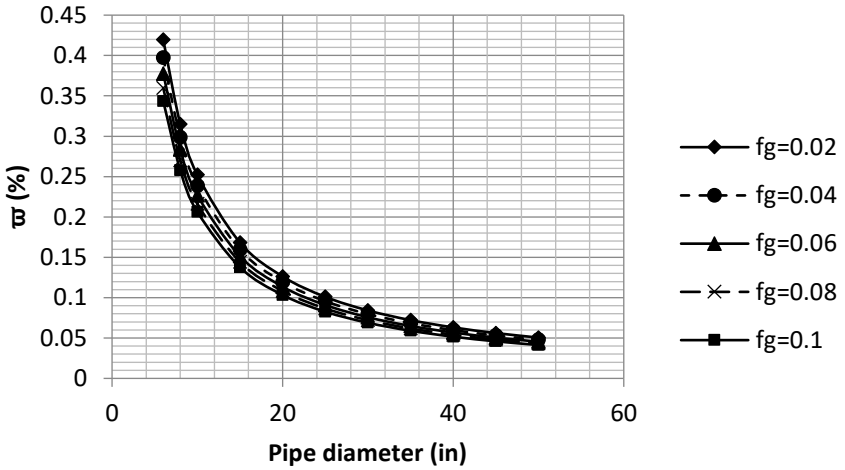

Fig. 4. Variation of ϖ with pipe diameter at different gas friction factor values.

Figure 5 shows the variation of the percentage contribution of pressure drop due to acceleration to the total pressure drop with pipe diameter at different solid volumetric concentration values. Again, a generally inverse relationship can also be noticed between the percentage contribution of pressure drop due to acceleration to the total pressure drop and pipe diameter. From the analysis of the model in equation (39), the total pressure drop increases with an increase in solid concentration, similar to the works of Tripathi et al. [21], Kumar et al. [22], Ulusarslan and Teke [23], Hamad et al. [18] and Saleh and Al-Byatti [19]. However, a critical look at the model shows that the component of the total pressure drop due to acceleration decreases with increasing solid concentration. In contrast, the friction component increases with an increase in solid concentration. Hence the overall increase in the total pressure drop is mainly influenced by the friction component of the total pressure drop when solid concentrations increase. It is, therefore, evident from Figure 5 that the effect of pipe diameter on the percentage contribution of pressure drop due to acceleration to the total pressure drop is equally influenced by the solid concentration. The influence of the solid concentration is better felt at lower solid concentrations than at higher concentrations. Specifically, at solid concentrations lower than 15%, there were sharp reductions in the percentage contribution of pressure drop due to acceleration to the total pressure drop as pipe diameter increased. But from 15% solid

concentrations, there was no distinguishable influence of the solid concentration. This can be explained by the fact that at lower solid concentrations, due to buoyancy effects, the velocity of the flowing gas is usually sufficient to carry all entrained solids. But as the solid concentration increases at a constant flow rate, the total mass of the transported mix also increases. This ultimately reduces the acceleration and the pressure drop due to acceleration since an inverse relationship exists between mass and acceleration. At higher solid concentrations, the particles tend to settle at the bottom of the pipe and do not significantly contribute to pressure drop due to acceleration.

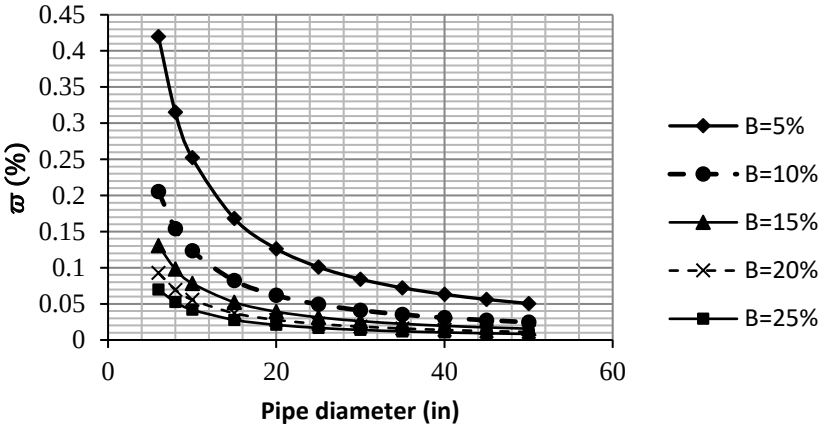

Fig. 5. Variation of ϖ with pipe diameter at different solid volumetric concentration values.

Figure 6 shows the variation of the percentage contribution of pressure drop due to acceleration to the total pressure drop with pipe length at different solid volumetric concentration values. The graph shows a generally inverse relationship between the percentage contribution of pressure drop due to acceleration and the total pressure drop and pipe length. The percentage contribution of pressure drop due to acceleration to the total pressure drop decreased as pipe length increased. This is explainable by the fact at a constant flow rate, longer pipes suffer from more frictional pressure drop at the pipe wall, thereby leading to a loss in flow velocity and pressure drop due to acceleration. But for shorter pipes, the loss in pressure is considerably lower, so the flow velocity remains high enough for a significant pressure drop. This reduction in the acceleration component of the total pressure drop as the length of the pipe increased is in good agreement with the works of Tripathi et al. [21] and Kuang et al. [24]. In addition, the solid concentration also influences the variation between the percentage contribution of pressure drop due to acceleration to the total pressure drop and pipe length. From the Figure 6, the reduction in the percentage contribution of pressure drop due to acceleration to the total pressure drop was faster for solid concentrations lower than 15%. Beyond this threshold, the influence of solid concentration remained relatively constant.

Figure 7 shows the variation of the percentage contribution of pressure drop due to acceleration to the total pressure drop with solid volumetric concentration at different solid-gas density ratios. The range of values for the ratio ρ_s/ρ_g was based on the average natural gas and sand density values. Apart from the inverse relationship between the percentage contribution of pressure drop due to acceleration to the total pressure drop and solid concentration, solid-gas density ratios equally affect the percentage contribution of pressure drop due to acceleration to the total pressure drop. The increase in solid concentration by weight is proportional to an increase in solid density. Hence, an increase in solid density (solid loading ratio) also increases the total pressure drop. These results compare favorably with other published works in the open literature [18, 19, 21–23]. However, a critical look at equation 39 shows that an increase in the solid-gas density ratio did not affect the acceleration component of the total pressure drop. However, the friction component of the total pressure drop increased with the solid-gas density ratio, thereby resulting in an increase in the total pressure drop. Therefore, the increase in the total pressure drop due to the increase in the solid-to-gas density ratio is mainly due to the increase in the friction component. Nonetheless, the percentage contribution of pressure drop due to acceleration to the total pressure drop decreased as the solid-to-gas density ratio (or solid loading ratio) increased. From the Figure 7, it can be deduced that at lower solid-gas density ratios, the effect of solid concentration on the percentage contribution of pressure drop due to acceleration to the total pressure drop was higher compared to higher solid-gas density ratios. Since density is directly proportional to mass, higher solid-gas density ratios mean higher transported solid mass. Since acceleration is inversely proportional to mass, higher transported total mass for a fixed gas velocity ultimately

leads to reduced pressure drop due to acceleration. This result is in good agreement with the works of Tripathi et al. [21] and Lin et al. [25]. Specifically, solid-gas density ratios significantly affected the percentage contribution of pressure drop due to acceleration to the total pressure drop at a solid-gas density ratio below 3000. Above this ratio, the effect of the solid-gas density ratio remained relatively constant.

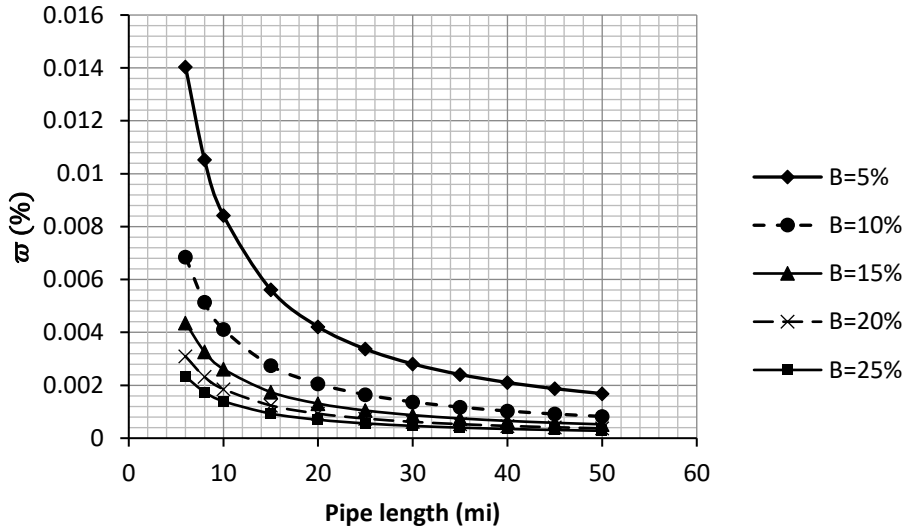

Fig. 6. Variation of ϖ with pipe length at different solid volumetric concentration values.

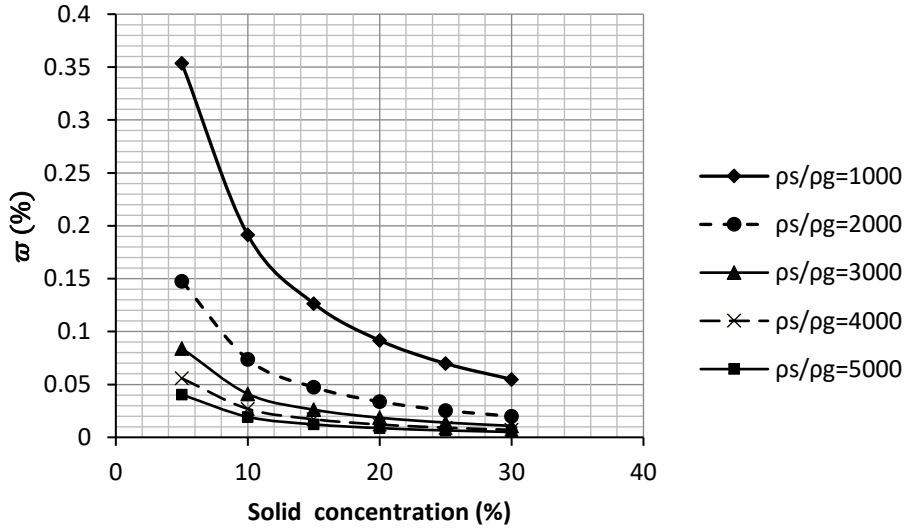

Fig. 7. Variation of ϖ with solid volumetric concentration at different solid-gas density ratios.

4. CONCLUSIONS

A new model for determining the total pressure drop of a two-phase gas–solid flow in horizontal pipes has been developed. The results of this study show that the acceleration component of the total pressure drop in a dilute solid phase-gas flow in a horizontal pipe is generally less than 1 %. This result is similar to the findings of Demneh and Mesbah [26], who reported that the realistic percentage contribution of pressure drop due to acceleration to the total pressure drop is less than 1%. The model for the gas-solid pipe system should be further validated with field or experimental data. From this study, the following conclusions can be reached:

(a) The total pressure drop increases with solid concentration, solid – gas density ratios and decreases with an increase in pipe diameter;

(b) An inverse relationship exists between the percentage contribution of pressure drop due to acceleration to the total pressure drop and pipe diameter, pipe length, solid concentration, and solid-gas density ratios, respectively;
(c) The gas friction factor showed an insignificant influence on the pressure drop due to acceleration to the total pressure drop;
(d) There exists a threshold beyond which the effect of solid concentration on the pressure drop due to acceleration to the total pressure drop for a gas-solid system remains largely constant;
(e) The influence of the dilute solid phase on the pressure drop due to acceleration in a gas-solid pipe system is insignificant (less than 1%).

REFERENCES

[1] Vatani, M., Ganji, D., Experimental examination of gas-liquid two-phase flow patterns in an inclined rectangular channel with 90 bend for various vertical lengths, International Journal of Engineering, Transactions A: Basics, vol. 35, no. 4, 2022, p. 685-691.
[2] Bello, K., Oycnken, B., Experimental investigation of sand transport velocity in multiphase fluid flow in pipes, Nigeria Journal of Technology, vol. 35, no. 3, 2016, p. 531-536.
[3] Santo, N., Portnikov, D., Tripathi, N., Kalman, H., Experimental study on the particle velocity development profile and acceleration length in horizontal dilute phase pneumatic conveying systems, Powder technology, vol. 339, 2018, p. 368-376.
[4] Fajemidupe, O.T., Aliyu, A.M., Baba, Y.D., Archibong, A.E., Okeke, N.E., Ehinmowo, A.B., Yeung, H., Minimum sand transport conditions in gas-solid-liquid three-phase stratified flow in horizontal pipelines, Proceedings of Nigeria Annual International Conference and Exhibition held in Lagos, Nigeria, 5–7 August 2019.
[5] Safikhani, H., Esmaeili, F., Salehfard, S., Numerical study of flow field in new design dynamic cyclone separators, International Journal of Engineering, IJE TRANSACTIONS B: Applications, vol. 33, no. 2, 2020, p. 357-365.
[6] Yan, Y., Haoping, P., Chuang, W., Sand transport and deposition behavior in subsea pipelines for flow assurance. PhD Thesis, School of Petroleum Engineering Chanzhu University, Wujin District, Changzhou, China, 2019.
[7] Bratland, O., Pipe flow 2: Multiphase flow assurance, (2ed), Dr OveBratland System Pte. Limited, 2013.
[8] Nabil, T., El-Sawaf, I., Elnahas, K., Computational fluid dynamics simulation of solid- liquid slurry flow in pipeline, Proceedings of the 17th International Water Technology Conference, Istanbul, 2013.
[9] Zhi-Gang, W., Chao-Yu, Y., Meng-Da, J., Jian-Fei, S., Yao-Dong., Experimental analysis of pressure characteristics of catalyst powder flowing down a cyclone dipleg, Journal of Petroleum Science, vol. 13, no. 2, 2016, 348-357.
[10] Trahan, J., Graziani, A., Goswami, D., Stefanakos, E., Jotshi, C., Goel, N., Evaluation of pressure drop and particle sphericity for an air-rock bed thermal energy storage system, Energy Procedia, vol. 57, 2014, p. 633 – 642.
[11] Ouyang, L., Aziz, K., Steady state gas flow in pipes, Journal of Petroleum Science and Engineering, vol. 14, 1996, p. 137-158.
[12] Agarwal, AT., Theory of design of dilute phase pneumatic conveying systems, Journal of Powder Handling and Processing, vol. 17, no. 1, 2005, p. 6-8.
[13] Tripathi, N., Sharma, A., Mallick, S., Wypych, P.W., Energy loss at bends in the pneumatic conveying of fly ash, Journal of Particuology, vol. 21, 2015, p. 65-73.
[14] Okafor, N.A., Aimikhe, V.J., Kinigorna, B., Modeling the effect of acceleration term on total pressure drop in horizontal gas pipelines, Petroleum and Coal, vol. 61, no. 6, 2019, p. 1314-1320.
[15] Liu, H., Pipeline engineering, Lewis Publishers, Boca Raton, London, New York, Washington, D.C., 2005.
[16] Ikoku, C.U., Natural gas engineering, Krieger Publishing Company Malabar, Florida, 1992.
[17] Orterga-Rivas, E., Unit operations of particulate solids: theory and practice. CRC PRESS. London, UK, 2012.
[18] Hamad, F.A., Faraji, F., Santim, C.G.S., Basha, N., Ali, Z., Investigation of pressure drop in horizontal pipes with different diameters, International Journal of Multiphase Flow, vol. 91, 2017, p. 120-129.
[19] Saleh, T.A., Al-Byatti, D.M.A., Experimental studies of pressure drop during multiphase flow (water, air and sand) in horizontal pipes, Nahrain University College of Engineering Journal, vol. 15, no. 1, 2012, p. 108-120.
[20] Santos, S.M., Tambourgi, E.B., Fernandes, F.A.N., Moraes Júnior, D., Moraes, M.S., Dilute –phase pneumatic coneying of polystyrene particles: pressure drop curve and particle distribution over the pipe cross-section, Brazilian Journal of Chemical Engineering, vol. 28, no. 1, 2011, p. 81-88.
[21] Tripathi, N.M., Levy, A., Kalmana, H., Acceleration pressure drop analysis in horizontal dilute phase pneumatic conveying system**,** Powder Technology, vol. 327, 2018, p. 43-56.

[22] Kumar, S., Singh, M.K., Ratha, D.N., Sandhu, H., Prasad, S.B., Effect of solid concentration on pressure drop characteristics in slurry pipeline using CFD, AIP Conference Proceedings, vol. 2341, no. 1, 2021.
[23] Ulusarslan, D., Teke, I., Relation between the friction coefficient and re number for spherical capsule train-water flow in horizontal pipes, Journal of Particulate Science and Technology, vol. 27, 2009, p. 488-495.
[24] Kuang, S., Zhou, M., Yu, A., CFD-DEM modelling and simulation of pneumatic conveying: a review, Powder Technology, vol. 365, 2020, p. 186–207.
[25] Lin, W., Li, L., Wang, Y., Pressure drop and particle settlement of gas–solid two-phase flow in a pipe, Applied Science, vol. 12, 2022, p. 1623.
[26] Demneh, F.A., Mesbah, A., The effect of kinetic energy change on flow in gas pipelines.The significance of the acceleration term in pressure drop calculations is investigated, Hydrocarbon Processing, 2008, p. 1-4.

Appendix

Table 1. Variation of ϖ with pipe diameter at different gas friction factor values.

	ϖ (%)				
D (in)	f=0.02	f=0.04	f=0.06	f=0.08	f=0.1
6	0.419557	0.397541	0.377720	0.359782	0.343470
8	0.314998	0.298452	0.283558	0.270079	0.257824
10	0.252158	0.238904	0.226975	0.216180	0.206365
15	0.168247	0.159397	0.151431	0.144224	0.137672
20	0.126238	0.119595	0.113616	0.108207	0.103289
25	0.101016	0.095699	0.090914	0.086584	0.082649
30	0.084194	0.079762	0.075773	0.072164	0.068883
35	0.072175	0.068375	0.064955	0.061861	0.059049
40	0.063159	0.059833	0.056840	0.054133	0.051671
45	0.056145	0.053189	0.050528	0.048121	0.045933
50	0.050533	0.047872	0.045478	0.043311	0.041341

Table 2. Variation of ϖ with pipe diameter at different solid volumetric concentration values.

	ϖ (%)				
D (in)	$\beta = 0.05$	$\beta = 0.1$	$\beta = 0.15$	$\beta = 0.2$	$\beta = 0.25$
6	0.419557	0.205171	0.130591	0.092687	0.069745
8	0.314998	0.153957	0.097975	0.069532	0.052318
10	0.252158	0.123204	0.078396	0.055633	0.041859
15	0.168247	0.08217	0.052277	0.037096	0.02791
20	0.126238	0.06164	0.039213	0.027824	0.020934
25	0.101016	0.049318	0.031373	0.022261	0.016748
30	0.084194	0.041102	0.026146	0.018551	0.013957
35	0.072175	0.035232	0.022411	0.015901	0.011963
40	0.063159	0.030829	0.01961	0.013914	0.010468
45	0.056145	0.027405	0.017432	0.012368	0.009305
50	0.050533	0.024665	0.015689	0.011132	0.008375

Table 3. Variation of ϖ with pipe length at different solid volumetric concentration values.

	ϖ (%)				
L (mi)	$\beta = 0.05$	$\beta = 0.05$	$\beta = 0.05$	$\beta = 0.05$	$\beta = 0.05$
6	0.014042	0.006853	0.004359	0.003092	0.002326

8	0.010532	0.005140	0.003269	0.002319	0.001745
10	0.008426	0.004112	0.002615	0.001855	0.001396
15	0.005617	0.002741	0.001743	0.001237	0.000931
20	0.004213	0.002056	0.001308	0.000928	0.000698
25	0.003370	0.001645	0.001046	0.000742	0.000558
30	0.002809	0.001371	0.000872	0.000618	0.000465
35	0.002408	0.001175	0.000747	0.000530	0.000399
40	0.002107	0.001028	0.000654	0.000464	0.000349
45	0.001873	0.000914	0.000581	0.000412	0.000310
50	0.001685	0.000822	0.000523	0.000371	0.000279

Table 4. Variation of ϖ with solid volumetric concentration at different solid-gas density ratios.

	ϖ (%)				
β (%)	$\frac{\rho_s}{\rho_g} = 1000$	$\frac{\rho_s}{\rho_g} = 2000$	$\frac{\rho_s}{\rho_g} = 3000$	$\frac{\rho_s}{\rho_g} = 4000$	$\frac{\rho_s}{\rho_g} = 5000$
5	0.353751	0.147700	0.084194	0.055789	0.040348
10	0.191448	0.073807	0.041102	0.026957	0.019388
15	0.126554	0.047338	0.026146	0.017087	0.012266
20	0.091617	0.03373	0.018551	0.012102	0.008680
25	0.069783	0.025441	0.013957	0.009095	0.006519
30	0.054846	0.019863	0.010878	0.007083	0.005075